The dynamics of self-similar consumer sprays

H. Hinterbichler*, H. Steiner, G. Brenn
Institute of Fluid Mechanics and Heat Transfer, Graz University of Technology, Austria
*Corresponding author: hannes.hinterbichler@tugraz.at

Introduction

Spray flows may assume self-similar behaviour on which the modelling of their dynamics can be built. Self-similar phenomena in sprays were reported in many different works. For example, Li and Shen [1] demonstrated self-similarity of the mean axial droplet velocity, produced in air-assisted atomization using a coaxial nozzle with a high-speed air stream in the inner tube. Others modelled the spray as a variable-density single-phase jet [2-4]. They obtained similar results for the velocity decrease along the spray axis as in the case of the free submerged single-phase jet. Karpetis and Gomez reported on self-similarity of the gaseous flow field and the evaporation source term in spray flames [5]. In all the mentioned works, liquid and gas were injected simultaneously, often resulting in no slip velocity between gas and drops from close to the nozzle and therefore endorsing self-similarity as observed for single-phase jets. Our work, instead, focuses on the flow field of a spray, where the motion of the gas phase is induced by the ejected liquid phase exclusively, since only liquid is ejected from the nozzle. We show that this particular flow also exhibits self-similarity, although the cross-sectional average gaseous momentum flow rate increases downstream, which is not the case for a single-phase jet [6]. In the region of the spray investigated, the flow dynamics is dominated by the interfacial drag force, promoting the momentum transfer from the liquid to the gaseous phase. The interfacial drag forces depend on the velocity slip between the two phases, which therefore needs to be accurately quantified in the computational modelling of the flow field. Measuring the velocity of the gaseous phase by PDA as represented by the small-droplets velocities is a non-trivial task, though. We do not discuss the details of this aspect of the study here.

We first present the materials and methods used in the experiments, then show and discuss some important measurement results characterising the sprays, and finally deduce the self-similar behaviour of the gas flow field in the sprays. The paper ends with the conclusions.

Materials and methods

We investigate experimentally sprays generated with a standard consumer-type nozzle at two different consumer spray-typical liquid mass flow rates, using phase-Doppler anemometry (PDA). The measurements are carried out at selected cross sections of the sprays located between approximately 40 and 450 nozzle diameters downstream from the nozzle. The spray can may be considered as a simple pressurized single-phase dispenser with an approximate nozzle orifice diameter of $D_{or} = 0.4$ mm. Water is used as the test liquid. Two different liquid mass flow rates $\dot{m}_l$ of 2 g/s and 2.92 g/s are investigated in our experiments. All the measurements are carried out at temperatures of 20±1°C.

The experimental setup is depicted on the left-hand side of figure 1. The nozzle is mounted on a two-axes traverse and supplied with liquid from a pressurized tank. The laser light source of the DANTEC PDA system is a continuous Argon-Ion laser (Coherent Innova 90C-3). Two pairs of intersecting laser beams with the wavelengths 488 nm and 514.5 nm, respectively, form coinciding probe volumes (figure 1, right). The axial and radial velocity components u_l and v_l, as well as the diameter d of drops passing the probe volumes are detected. The geometrical parameters of the PDA system and the measuring ranges for the droplet properties are listed in table 1 for both liquid mass flow rates.

The sprays are considered as axially symmetric. Therefore, the measurement points are arranged along one radial axis r in each cross section of the sprays (see right hand-side of figure 1). Measurements are taken in several cross sections of the sprays with axial distances z from the nozzle exit ranging from 15 to 150 mm for $\dot{m}_l = 2$ g/s, and 15 to 180 mm for $\dot{m}_l = 2.92$ g/s. These ranges of the axial distance correspond to values of $z/D_{or} = 38$ to 375, and $z/D_{or} = 38$ to 450, respectively. In order to ensure sufficient statistical reliability of the PDA measurements, 100,000 samples were acquired at each measurement point. The edge of the spray flow field was defined at a radial position, where the detected drop frequency was 5 % of the maximum detection rate in the current spray cross section, or at least 300 Hz.

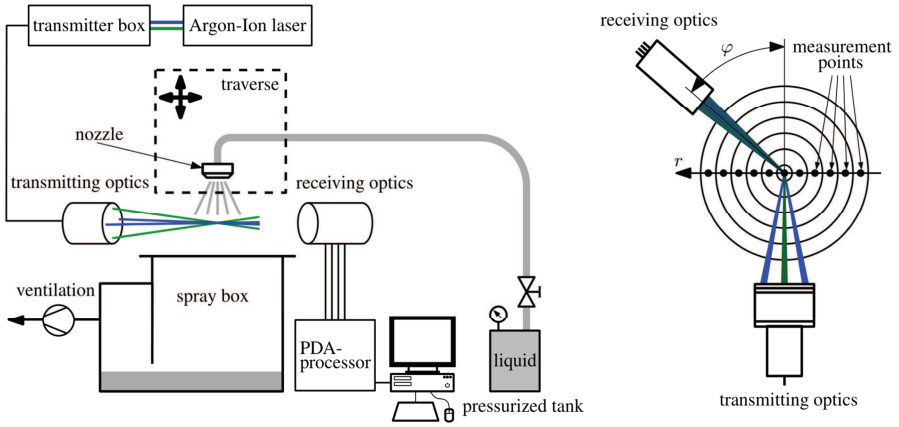

Figure 1. Experimental setup (left) and PDA optics (right).

Table 1. Geometrical parameters and measuring ranges of the PDA system.

PDA parameters	$\dot{m}_l = 2$ g/s	$\dot{m}_l = 2.92$ g/s
Scattering angle φ	50°	50°
Beam half angle	1.386°	1.386°
Phase factor P12	2.231°/µm	2.373°/µm
Phase factor P13	0.870°/µm	1.028°/µm
Measuring range d	up to 298 µm	up to 251 µm
Measuring range u_l	-63.8 to 63.8 m/s	
Measuring range v_l	-20.2 to 20.2 m/s	

Results and discussion

Spray properties

In the present section, exemplary mean quantities of the sprays are discussed. In figure 2, the mean droplet ter D_{10} and the mean axial drop velocity $\bar{u}_l$ are depicted for the liquid mass flow rates of $\dot{m}_l = 2$ g/s (left) and $\dot{m}_l = 2.92$ g/s (right). Due to the axial symmetry of the sprays, measurement points are concentrated on the positive half of the radial axis, whereas fewer points of measurement were placed on the negative half of the axis, mainly for checking symmetry. It can be seen for all displayed quantities that our assumption of axial symmetry is confirmed.

In the top row of figure 2, radial profiles of the arithmetic mean droplet diameter D_{10} are shown. For both cases, the smallest mean droplet diameters are found along the symmetry axis. The values increase towards the edge of the spray. This indicates that small droplets can be found rather in the dense region along the symmetry axis of the sprays, while larger drops with more inertia are found radially farther outwards. The mean drop diameter increases along the axis downstream, whereas the opposite is true in the radially outer regions of both sprays.

For the mean axial drop velocities $\bar{u}_l$ (see figure 2, bottom row), substantial differences between the two sprays generated at different liquid mass flow rates are observed. Whereas all profiles are rather bell shaped at the lower mass flow rate (left-hand side), two peaks in the mean axial velocity profile closest to the nozzle exit ($z = 15$ mm) are seen for the higher mass flow rate (right-hand side). Downstream, the profile shifts, and an additional third peak arises along the symmetry axis. The difference between the mean axial drop velocity profiles at the inflow of the two sprays may be attributed to the geometry of the nozzle and the state of flow. At larger flow rates, a hollow conical sheet is formed due to the swirl induced by the 90° redirection of the flow closely upstream from the nozzle exit.

Velocity of the gas flow field

Typically, the velocity of the gas flow field is deduced from PDA data under the assumption that the relaxation time scale of small droplets is very small, resulting in very small Stokes numbers. Therefore, the small droplets act like nearly massless tracer particles, representing the ambient gas flow field. This is especially true if the process of atomization is dominated by an independently imposed gas flow. However, for the present sprays the contrary is true.

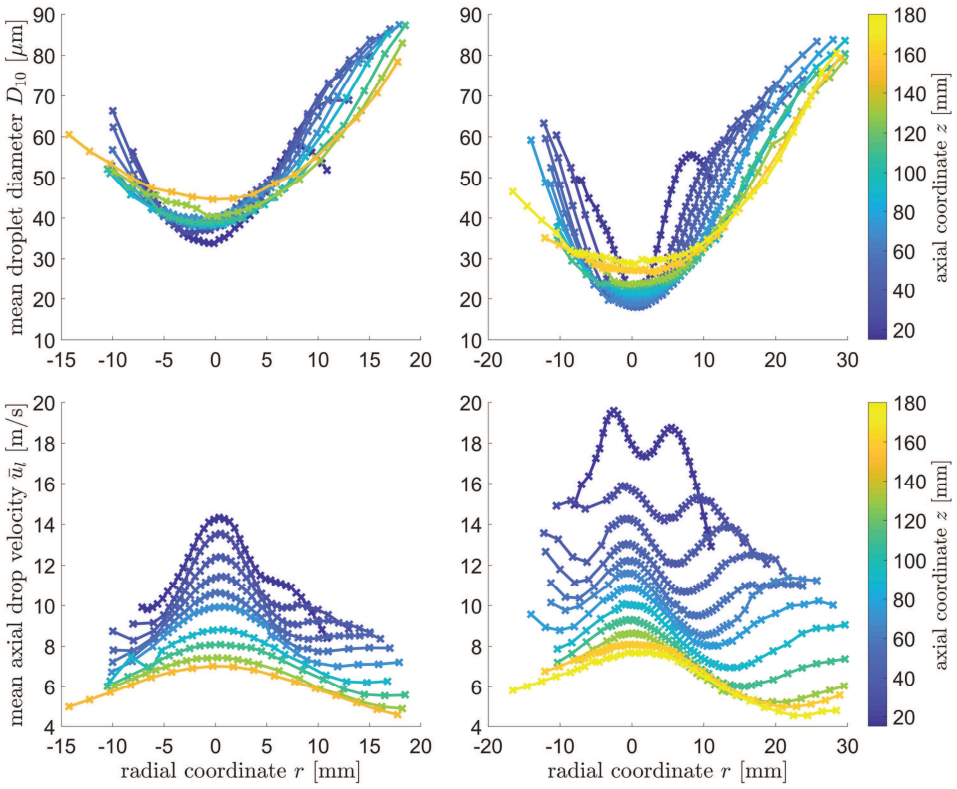

Figure 2. Experimentally measured spray properties: Left: $\dot{m}_l = 2$ g/s, right: $\dot{m}_l = 2.92$ g/s. Radial profiles of (top) number-mean drop size and (bottom) mean axial drop velocity.

Since only liquid is ejected from the nozzle, the gas phase is set into motion only due to the interaction with the droplets. Our measurements indicate that, especially in the cross sections close to the nozzle exit, not all small droplets act as tracer particles. A careful investigation shows that the velocity spectra of small droplets below 15 µm may be bimodal. For determining the gas velocity from the small droplet velocities, the drops forming the mode at the lower velocities must be used. Making use of for this we obtain gas velocity profiles as shown in figure 3.

Self-similar gas flow field

The analytical investigation of a possibly self-similar gas flow in the sprays assumes the flow field as a boundary layer-type flow. The corresponding boundary layer equations, with constant pressure in the flow field, transformed into a self-similar coordinate $\eta = Dr/(z - z_0)^{\alpha}$, with use of the stream function $\Psi = C(z - z_0)^{\beta}F(\eta)$ for the cylindrical flow field, yield the ordinary differential equation

$$(\beta - 2\alpha)F'^2 - \beta FF'' + \beta\frac{FF'}{\eta} = \frac{\nu}{C(z - z_0)^{\beta-1}}\eta\left[\eta\left(\frac{F'}{\eta}\right)'\right]' + \frac{E}{C^2D^4}\frac{\eta^2\omega_z}{(z - z_0)^{-4\alpha+2\beta-1-\gamma}} \qquad (1)$$

for the self-similar stream function $F(\eta)$, where the second term on the right represents the momentum source from the liquid phase $E(z - z_0)^{\gamma}\omega_z(\eta)$. The independence of z requires that $\beta = 1$ and $-4\alpha + 2\beta - 1 - \gamma = 0$. Determining the exponent α and the virtual pole of the flow z_0 by requiring that the ratio of the local axial velocity u in the flow field to the maximum value u_0 at $r = 0$ must be a constant along lines $\eta = \text{constant}$, and that the velocity along the symmetry axis $u_0(z)$ decreases $\propto (z - z_0)^{\beta-2\alpha}$, we get the values in table 2.

In figure 4 the normalized gas velocities are plotted as functions of the self-similar coordinate η divided by the constant D. The velocity profiles at various distances z from the nozzle exit collapse nicely on each other, showing the self-similar behaviour of the gas flow fields. The authors are presently working on the self-similar description of the momentum source from the liquid phase.

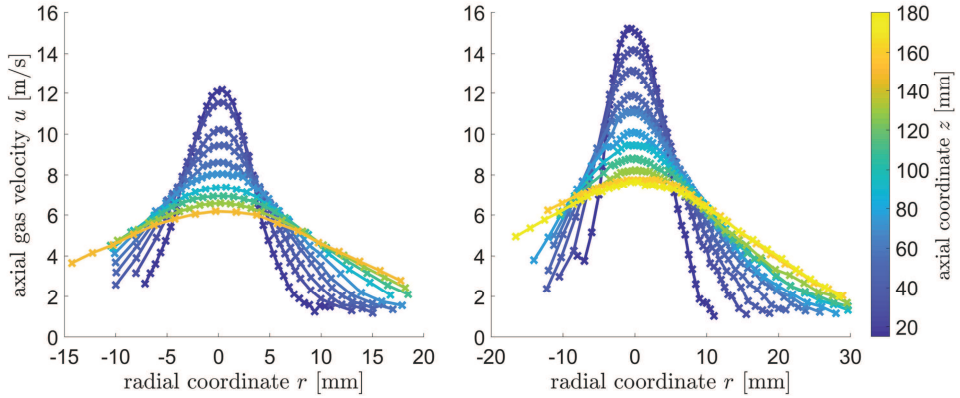

Figure 3. Axial velocity profiles of the gas flow field. Left: $\dot{m}_l = 2$ g/s, right: $\dot{m}_l = 2.92$ g/s.

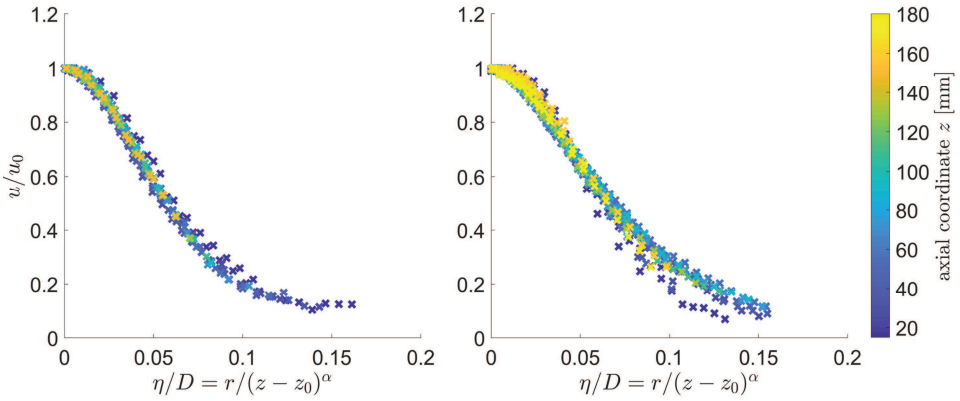

Figure 4. Self-similar profiles of the gas flow field. Left: $\dot{m}_l = 2$ g/s, right: $\dot{m}_l = 2.92$ g/s.

Table 2. Computed parameters to obtain a self-similar solution.

$\dot{m}_l$ [g/s]	2	2.92
α	0.67	0.70
z_0 [mm]	-2.5	-14.0

Conclusions

Consumer sprays were experimentally investigated with PDA at two different liquid mass flow rates relevant for the application. The measurements cover a region of the spray with large slip velocity between the liquid and the gaseous phases. We demonstrated a suitable approach to determine the velocity of the gaseous phase from PDA data, accounting for the bimodal velocity spectra observed for small droplets. This aspect was not detailed here. Furthermore, we show that the gas flow field of the spray can be represented in terms of self-similar variables, accounting for momentum transfer from the liquid to the gaseous phase. The observed decrease in the axial gas velocity with increasing downstream distance is significantly smaller than in a single-phase jet. Future tasks are the determination of the momentum source term from our PDA data and the solution of the self-similarity transform of the momentum equation.

References

[1] Li, X., Shen, J., Journal of Propulsion and Power 15: 103-110 (1999).
[2] Shearer, A.J., Tamura, H. Faeth, G.M., Journal of Energy 3: 271-278 (1979).
[3] Faeth, G.M., Progress in Energy and Combustion Science 9: 1-76 (1983).
[4] Panchagnula, M.V., Sojka, P.E., Fuel 78: 729-741 (1999).
[5] Karpetis, A.N., Gomez, A., Journal of Fluid Mechanics 397: 231-258 (1999).
[6] George, W.K., Advances in Turbulence (George and Arndt, eds): 39-73, Hemisphere, NY (1989).